KSME Journal, Vol. 10, No. 2, pp. 223~234, 1996

Numerical Simulation of Flows of Non-Newtonian Fluids in the Stenotic and Bifurcated Tubes

Sang-Sin Yoo*, Sang-Ho Suh and Hyung-Woon Roh****

(Received August 3, 1995)

Steady flows of Newtonian and non-Newtonian fluids in the stenotic and bifurcated tubes are numerically simulated. Four rheologically different fluids such as water, aqueous sugar solution, aqueous Carbopol solution and blood are selected for the numerical simulation and the modified power-law model is used for the numerical simulation of non-Newtonian fluids in the stenotic and bifurcated tubes. Apparent viscosity of a non-Newtonian fluid in the modified power-law model is expressed as a function of the shear rate. Flows in the circular tube with sudden contraction-sudden expansion and gradual contraction-gradual expansion are studied numerically. Analyses in the stenotic tubes are concentrated on the effects of rheological properties, the stenotic geometry and Reynolds number. Flow characteristics of Carbopol solution in the stenotic tubes are compared with those of blood. Effects of the bifurcation geometry on the flow behaviors of Newtonian and non-Newtonian fluids are numerically investigated. Numerical analyses are focused on the flow patterns in the branch tubes of which angles are 30°, 60° and 90° and on the diameter ratios for Newtonian and non-Newtonian fluids. Variations of the axial velocity and pressure drop along the bifurcated tubes for various flow parameters are presented for Newtonian and non-Newtonian fluids.

Key Words: Non-Newtonian Fluids, Modified Power-Law Model, Stenotic Tubes, Bifurcated Tubes, Numerical Flow Analysis

Nomenclature

D_{b1} : Diameter of first branch tube(m)
D_{b2} : Diameter of second branch tube(m)
D_0 : Diameter of circular tube in the upstream(m)
L : Length of stenotic section(m)
m : Consistency of power-law model(Pa·s^n)
n : Power-law index
p : Static pressure(Pa)
p_0 : Static pressure at the inlet(Pa)
R : Radius of stenotic section(m)
R_0 : Radius of circular tube(m)
r : Radial direction
t : Height of stenosis(m)
u : Axial velocity(m/s)
u_i : Velocity vector
U_0 : Average velocity in the upstream(m/s)
v : Radial velocity(m/s)
z : Axial direction

Greek Letters

$\dot{\gamma}$: Shear rate(s^{-1})
$\dot{\gamma}_o$: Cut-off shear rate(s^{-1})
μ_e : Apparent viscosity(Pa·s)
μ_0 : Zero shear rate viscosity(Pa·s)
θ : Bifurcation angle
ρ : Density(kg/m^3)
τ_{ij} : Shear stress tensor

* Dept. of Mech. Eng. & Design, Hankuk Aviation University
** Dept. of Mech. Eng., Soong Sil University

1. Introduction

Flow phenomena in the stenotic and bifurcated tubes are frequently encountered in the engineering piping systems and biomedical applications. Many experimental investigations and numerical works for flows of Newtonian fluids in the

stenotic and bifurcated tubes are reported in the literature. Only a few studies for the same geometry mentioned above are reported in the publications for non- Newtonian fluids (Banerjee, 1992; Cho and Kensey, 1991; Milnor, 1989; Morales and Campo, 1993; Nicols and O'Rourke, 1990; Yoo, 1993).

Aqueous polymer solutions are used as substitutes for human blood in the experimental studies due to complexity of blood for the experimental application. Polymer solutions behave quite differently from Newtonian fluids in tube flows showing rheological complexity. Proper constitutive equations for non-Newtonian fluids are required to present the experimental results and to solve the governing equations. Flow characteristics of non-Newtonian fluids in the odd geometries such as sudden contraction-sudden expansion, gradual contraction-gradual expansion, and bifurcation of tubes should be well investigated to understand the physical phenomena obtained in experimental results.

Flow phenomena in the bifurcated tubes are of significance for practical piping systems and biomedical applications (Lee and Goo, 1993). Due to complex geometry branch flow analyses of Newtonian and non-Newtonian fluids are relied on the numerical methods to predict general flow characteristics, and then experimental data are supplemented to verify the numerical analysis for the specified geometry. Most of flow studies in the bifurcation tubes are focused on the effects of the flow rate ratio and Reynolds number on the velocity distribution, pressure variation and wall shear stress for the bifurcation angle of 90° (Choi and Yoo, 1992; Khodadadi et. al., 1986; Liepsch et. al., 1982; Yung et. al., 1990). Only a few works are reported for the other bifurcated angles and rounding effects of the bifurcated region.

In this study numerical analyses are focused on flow patterns in the stenotic and bifurcated tubes for Newtonian and non-Newtonian fluids. Geometries of sudden contraction-sudden expansion and gradual contraction-gradual expansion are used for the stenotic section. Branch flows for the bifurcation models with branch angles of 30°, 60°, and 90° are analysed. Effects of the diameter ratio and the power-law index of non-Newtonian fluids are investigated.

2. Governing Equations

The following governing equations are used to obtain the flow characteristics of non-Newtonian fluids.

$$u_{j,j}=0 \tag{1}$$

$$\rho u_j u_{i,j} = -p_{,i} + \tau_{ij,j} \tag{2}$$

Equations (1) and (2) are continuity and momentum equations for 3-dimensional, steady, incompressible flows, respectively.

Among various constitutive equations the power-law model which is suitable and convenient for studying flow characteristics of non-Newtonian fluids is employed in the current study (Park and Lee, 1992; Suh and Yoo, 1993).

$$\tau = m\dot{\gamma}^n \tag{3}$$

where m and n are constants representing the rheological properties of a non-Newtonian fluid. The shear rate($\dot{\gamma}$) is defined as

$$\dot{\gamma} = \sqrt{\frac{1}{2}\left[\sum_i \sum_j \dot{\gamma}_{ij}\dot{\gamma}_{ji}\right]} \tag{4}$$

The local apparent viscosity of a non-Newtonian fluid can be determined from the power-law model, once the local shear rate is calculated (Chang et. al., 1993; Roh et. al., 1993).

The power-law model describes the rheological behavior of a non-Newtonian fluid quite well for the wide range of shear rates. However, the model predicts the apparent viscosity too high for the range of low shear rate. Therefore, it is necessary to modify the power-law model such a way that the apparent viscosity remains constant in very low range of the shear rate. The following formula is used to calculate the apparent viscosity of the power-law model.

$$\mu_e = \begin{cases} m\dot{\gamma}_0^{n-1}, & \dot{\gamma} < \dot{\gamma}_0 \\ m\dot{\gamma}^{n-1}, & \dot{\gamma} \geq \dot{\gamma}_0 \end{cases} \tag{5}$$

where $\dot{\gamma}_0$ is the cut-off shear rate defined for the modified power-law model.

Equation (3) is called the modified power-law

model when Eq. (5) is used for calculation of the apparent viscosity of a non-Newtonian fluid. Substituting Eq. (3) into Eq. (2), the momentum equation for a non-Newtonian fluid can be represented as follows :

$$\rho u_j u_{i,j} = -p_{,i} + \mu_e (u_{i,j} + u_{j,i})_{,j} \qquad (6)$$

3. Rheological Properties of Fluids

Many experimental studies concerned with substitutional fluids for human blood have been reported in the literature. Some fluids such as aqueous sugar solution (33w%) and aqueous Carbopol 934 solution (1.0w%) are chosen as the substitutive fluids for blood. The apparent viscosities of selected fluids are depicted in Fig. 1. Water and aqueous sugar solution are a typical Newtonian fluid, but the aqueous Carbopol solution is known as a typical purely viscous non-Newtonian fluid and blood as a slightly viscoelastic non-Newtonian fluid with yield stress.

The rheological characters of blood and aqueous Carbopol solution are represented by the power-law model in Fig. 1 (Banerjee, 1992). Solid line and dotted line in Fig. 1 depict the rheological characters of blood and Carbopol solution, respectively. In the lower range of shear rate the apparent viscosity of the sugar solution is quite different from that of blood, but the apparent viscosity of Carbopol solution is very similar to that of blood. However, the apparent viscosity of both Carbopol solution and sugar solution in the high rate of shear are quite similar to that of blood, especially around the shear rate order of 10^2. The apparent viscosity of blood changes more significantly than other fluids as the shear rate increases.

Aqueous Carbopol solution shows more similar rheological character to blood than aqueous sugar solution for wide range of shear rate. Parameters for the rheological character of four fluids are presented in Table 1, where m and n are consistency and power-law index of the modified power-law model, respectively.

4. Numerical Analyses

For numerical simulation of steady, two-dimensional, incompressible flows in the stenotic tubes, the governing equations are converted into non-linear algebraic equations by the Galerkin method, and then the equations are linearized by the fixed point iteration method or the quasi-Newton method and finally the resulting equations are solved by using the Gaussian elimination method. The FIDAP code prepared by FDI (Fluid Dynamic International) is used to solve the flows in the stenotic tubes (Chang et. al., 1993).

The finite volume predictions in bifurcated tubes were obtained by using a $35 \times 10 \times 10$ grid, body-fitted coordinate system and hybrid differencing scheme. The SIMPLE-C (Semi-Implicit Method for Pressure Linked Equations-Consistency) is applied to pressure and velocity corrections. The STONE method is used to

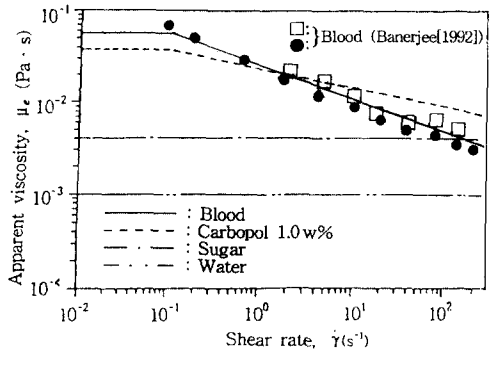

Fig. 1 Apparent viscosity versus shear rate for rheologically different fluids

Table 1 Properties of four different fluids (Cho et. al., 1985 ; Pak et. al., 1990)

Properties / Fluids	ρ(kg/m^3)	m(Pa·s^n)	n	μ_0(Pa·s)
Water	1000	0.001	1.00	0.001
Aqueous 33w% sugar solution	1142	0.004	1.00	0.004
Aqueous 1.0w% carbopol solution	1004	0.023	0.80	0.037
Blood	1050	0.027	0.53	0.056

obtain the iterative solutions of the finite volume discretization equations. In the computer code the pressure boundary condition which specifies $p=0$ and $\partial u_i/\partial x=0$ is applied for the outlet boundary condition. The constitutive equation, Eq. (5), is used to calculate the apparent viscosity of non-Newtonian fluids. In the user subroutine of Fortran program the calculation of Eq. (5) is directly connected to the solver. In this manner, once the local shear rate is calculated the apparent viscosity of non-Newtonian fluids can be determined in the numerical analysis. The FLOW3D release 3.2.1 code developed by AEA(Atomic Energy Authority) is used to simulate the branch flows of non-Newtonian fluids. The code consists of three modules, such as Pre-processor (SOPHIA), Solver (FLOW3D) and Post-processor (JASPER)(Roh et. al., 1993). User's subroutine for calculation of apparent viscosity is programmed to connect with FLOW3D codes. The relative error to velocity in convergence criteria is 1×10^{-6}.

CONVEX C120 and SUN SPARCstation IPC are used for numerical simulation, and the results are down-loaded to a SUN SPARCstation IPC workstation.

5. Flow in the Stenotic Tubes

Geometric configuration of a stenotic tube is shown in Fig. 2. Dotted lines in the figure depict the sudden contraction-sudden expansion shape and solid line shows the cosine curved shape of Eq. (7).

$$R(\ell)=R_0-\frac{t}{2}\left\{1+\cos\frac{\pi\ell}{(L/2)}\right\} \tag{7}$$

where R_0, t, and L are radius of circular tube, height of stenosis and length of stenotic section respectively.

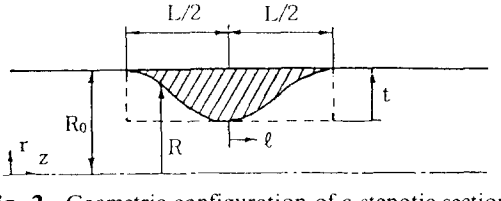

Fig. 2 Geometric configuration of a stenotic section

For Numerical computation of flows in the stenotic tube, the height and length of the stenosis are set to be $t=R_0/2$ and $L=2R_0$.

5.1 Newtonian and non-Newtonian fluids in the stenotic tubes

For Reynolds number of 50 and fully developed flow from the inlet section, streamlines in the circular tube with stenotic section are shown in Fig. 3 for rheologically different fluids. The reattachment length of water in the downstream side of the stenotic section is the longest among fluids, while aqueous sugar solution, aqueous Carbopol solution and blood show shorter reattachment lengths in order. Non-Newtonian fluids such as blood and aqueous Carbopol solution show shorter reattachment length than a Newtonian fluid.

Variations of velocity and pressure along the centerline are presented for the fully developed flow and $Re=50$ in Figs. 4 and 5, respectively. The results are presented in terms of dimensionless parameters such as z/D_0, u/U_0 and $(p-p_0)/0.5\rho U_0^2$, where u and p are the centerline velocity and pressure at z from the inlet, respectively. The average velocity U_0 and inlet pressure p_0 are used for the reference quantities.

In the upstream of the stenosis the centerline velocities of blood and aqueous Carbopol solution are smaller than those of water and sugar

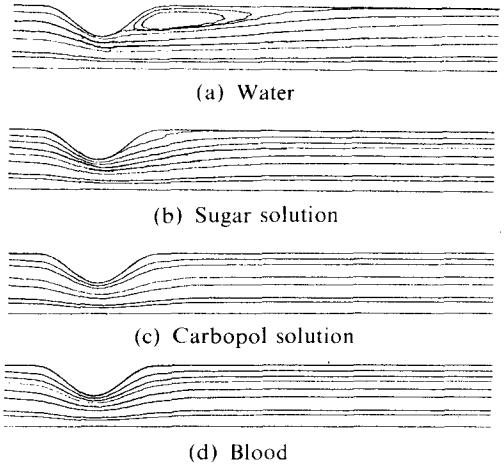

Fig. 3 Streamline contours in the stenotic tube at Re = 50

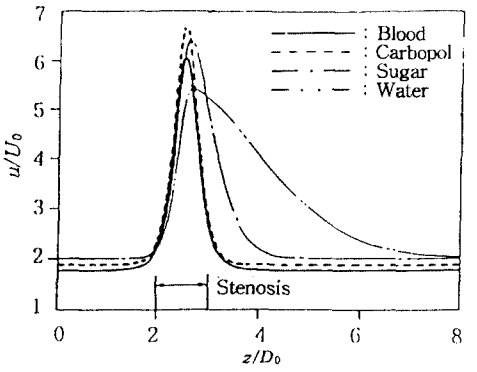

Fig. 4 Variation of the centerline velocity in the stenotic tube at Re=50

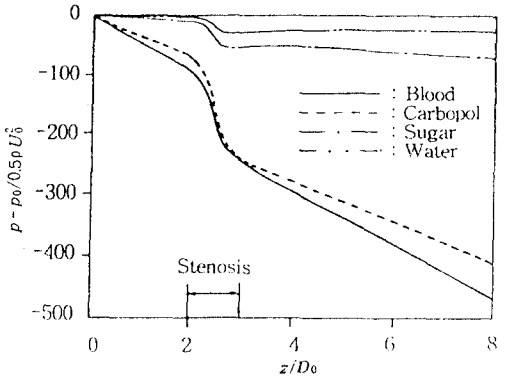

Fig. 5 Pressure drop along the axis in the stenotic tube at Re=50

solution. This is mainly due to the fact that the velocity profile of a non-Newtonian fluid in the fully developed flow is flatter in the central region than that of a Newtonian fluid. Passing through the stenotic section the velocity of a fluid changes rapidly. Centerline velocities of water and sugar solution are the same in the upstream side of the stenosis. However, the velocity of sugar solution in the stenotic section is quite different from that of water, showing higher velocity for sugar solution than for water. Four different fluids exhibit quite different velocity patterns in the stenotic section and downstream side of the stenosis. Aqueous Carbopol solution shows the highest centerline velocity in the stenotic section, while water shows the lowest velocity.

It is clear that the apparent viscosity and rheological characteristics of a fluid play significant roles in the stenotic section. The centerline velocity decreases rapidly passing through the stenosis; blood and Carbopol solution resume their fully developed values shortly in the downstream side, while water shows the longest distance to reach its fully developed value. Far downstream side from the stenosis all fluids resume their fully developed patterns just as those in the upstream side.

Pressure drops of blood and Carbopol solution along the axis are much larger than those of water and sugar solution in the upstream, at the stenosis and in the downstream side. It is apparent that the viscosity plays the major role on the pressure drop for a Newtonian fluid and the apparent viscosity for non-Newtonian fluids. Pressure drop of blood along the axis in the upstream and downstream sides of the stenosis are larger than that of Carbopol solution. The larger pressure drop of non-Newtonian fluids in the stenotic section is related to high value of the apparent viscosity gradient of non-Newtonian fluids in the flow field.

For $Re=400$ and fully developed flow from the inlet section, the centerline velocity and pressure drop along the axis are shown in Fig. 6 and Fig. 7, respectively. Blood and Carbopol solution resume their respective fully developed velocity profiles much faster than water and sugar solution. It is attributed to the fact that the rheological characters of fluids are quite different in the flow field. The apparent viscosities of blood and

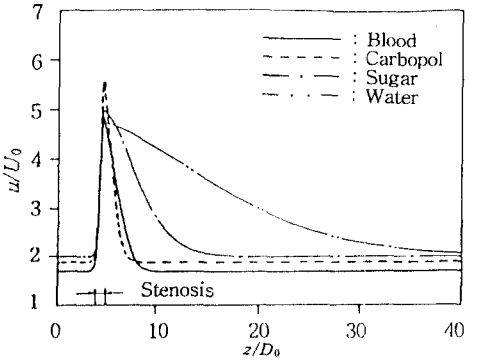

Fig. 6 Variation of the centerline velocity in the stenotic tube at Re=400

Carbopol solution for the range of the shear rate experienced in the flow field are much higher than those of water and sugar solution and the power-law index of those fluids are much lower than a Newtonian fluid.

Pressure drops across the stenotic section at $Re=400$ for non-Newtonian fluids are quite different from those at $Re=50$ showing very strong Reynolds number dependency. Dimensionless pressure drop of fluids decreases as Reynolds number increases. An abrupt pressure drop due to the stenotic section is shown in Fig. 7.

The static pressure decreases to the lowest local value just after the stenotic section, recovers gradually from the minimum, reaches its local maximum and finally, decreases linearly in the far downstream. Pressure drop of Carbopol solution along the axis is much higher than that of blood at $Re=400$, which is contrary to the results obtained at $Re=50$. The higher pressure drop of Carbopol solution at $Re=400$ is caused by high value of the apparent viscosity in the flow field. The apparent viscosity of Carbopol solution is higher than that of blood in the high range of the shear rate as shown in Fig. 1.

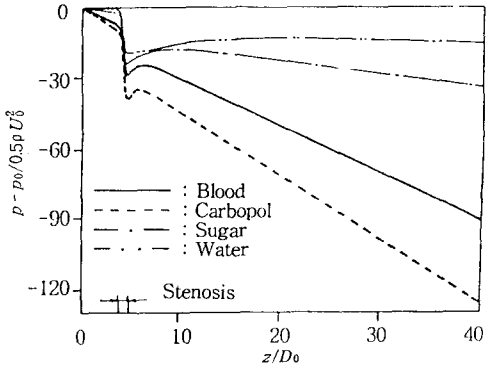

Fig. 7 Pressure drop along the axis in the stenotic tube at Re=400

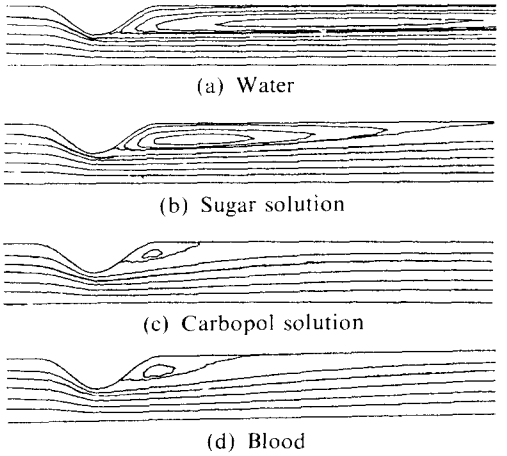

Fig. 8 Streamline contours in the stenotic tube at Re =400

Streamlines along the stenotic tube at $Re=400$ is shown in Fig. 8. The recirculating zone of Carbopol solution is smaller than that of blood, representing the shorter reattachment length of Carbopol solution. By comparison of Figs. 3 and 8, it can be shown that the recirculating zone and the reattachment length increase as Reynolds number increases.

5.2 Blood flow in the stenotic tubes

Rheological property of blood is represented by the modified power-law model and effects of the stenotic shapes and Reynolds numbers on the blood flow in the stenotic tubes are numerically analysed. Centerline velocity and pressure drop along the axis for blood are shown in Figs. 9 and 10, respectively. S.C.-S.E. and G.C.-G.E. in the figures depict the sudden contraction-sudden expansion and gradual contraction-gradual expansion, respectively.

For the same Reynolds number the centerline velocity in the S.C.-S.E. tube is much higher than

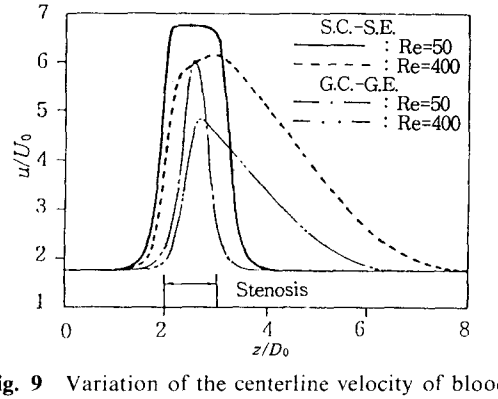

Fig. 9 Variation of the centerline velocity of blood in the circular tubes with different stenotic sections

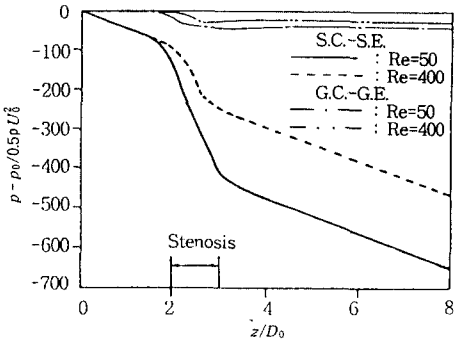

Fig. 10 Pressure drop of blood along the axis in the circular tubes with different stenotic sections

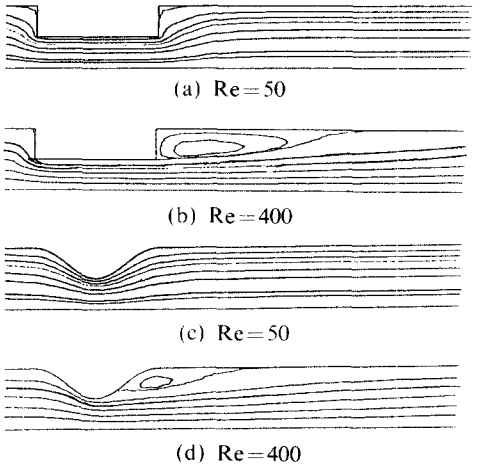

Fig. 11 Streamline contours of blood in the circular tubes with different stenotic sections

that in the G.C.-G.E. tube. This phenomenon occurs for all Reynolds numbers. Reattachment length of the blood flow increases as Reynolds number increases. Longer reattachment length for high Reynolds number is analogous to the longer hydrodynamic entrance length for high Reynolds number of non-Newtonian fluids. Reattachment length in the S.C.-S.E. tube is longer than that in the G.C.-G.E. tube, regardless of Reynolds number.

Obviously, pressure drop in the S.C.-S.E. tube is larger than that in the G.C.-G.E. tube. The orders of magnitude of the pressure drops in the S.C.-S.E. and G.C.-G.E. tubes are quite different. Streamline contours around the stenotic sections for blood are presented in Fig. 11. For the same Reynolds number the recirculating zone and the reattachment length in the S.C.-S.E. tube are much larger than those in the G.C.-G.E. tube. The geometric configuration of a stenotic tube should be carefully examined for practical application of the blood flow.

6. Flow in the Bifurcation Geometry

In the present numerical study rheological characters of blood and Carbopol solution are modeled by the modified power-law model to account for the apparent viscosity in the lower range of shear rate by introducing the cut-off shear rate. It is observed that the velocity distribution and pressure drop along the axis are not much affected by the value of the cut-off shear rate in the low range of shear rate. Therefore, the cut-off shear rate is selected to $\dot{\gamma}_0=0.1$ for numerical calculation.

Schematic configuration of a bifurcated tube is shown in Fig. 12. Main tube D_0 in the upstream is bifurcated into two branches symmetrically, diameter D_{b1} for one branch and D_{b2} for the other. This bifurcated configurations may be found in the industrial piping systems, femoral artery and abdominal aorta of the human body.

6.1 Effect of the bifurcation angle

For Reynolds number of 400 and diameter ratio $D_{b1}/D_0=1.0$, the centerline velocity and pressure variation along the axis of a Newtonian fluid are shown in Figs. 13 and 14, respectively.

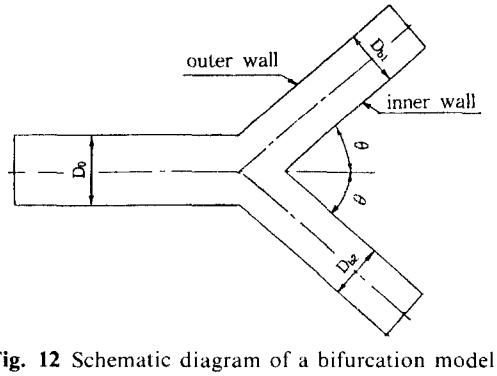

Fig. 12 Schematic diagram of a bifurcation model

Abbreviation B.P. in the figures depicts the bifurcation point. Dimensionless parameters are defined based on the quantities of main tube, such as z/D_0, u/U_0 and $\Delta p/(0.5\rho U_0^2)$. Diameter D_0 and average velocity U_o in the main tube are used for the reference quantities. Axial location along the centerline is denoted by z and the pressure difference between inlet value and local value by Δp.

Centerline velocities of fluids in the upstream side where the fully developed flow from the entrance of tube prevails are all identical regardless of the bifurcation angles. However, the centerline velocity decreases sharply in the bifurcated region depending upon the bifurcation angle. A steeper decrease of the velocity occurs for the highest bifurcation angle. The larger the bifurcation angle, the steeper the variation of velocity in the bifurcation region. Recovering phenomenon of velocity from the lowest value in the bifurcated region is similar for all bifurcation angles. Velocities in the far downstream side of the daughter branch resume their fully developed pattern.

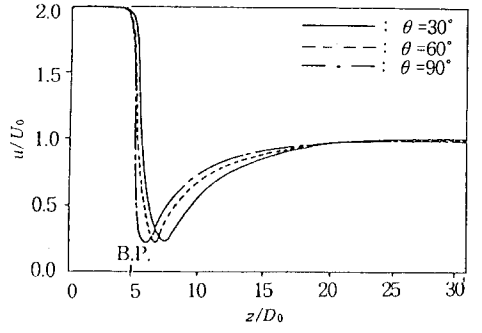

Fig. 13 Effect of the bifurcated angle on the centerline velocity for a Newtonian fluid

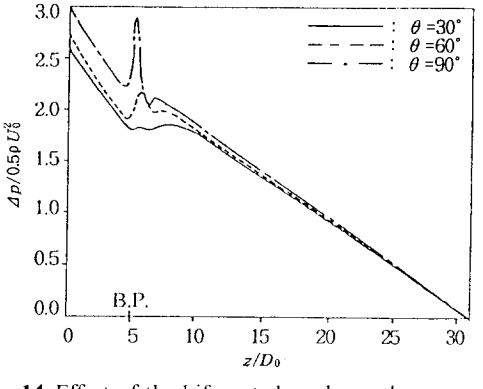

Fig. 14 Effect of the bifurcated angle on the pressure along the axis for a Newtonian fluid

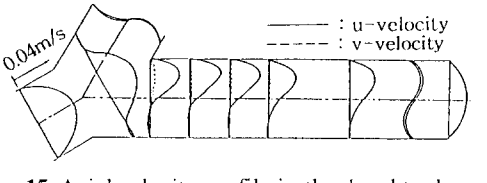

Fig. 15 Axial velocity profile in the daughter branch with the bifurcation angle of 30°

The centerline pressures in the main tube and downstream side of the branch show the fully developed patterns. However, the pressure in the bifurcated region is strongly affected by the bifurcation angle, showing very irregular flow phenomenon due to abrupt change in flow direction and area.

Figure 15 shows the axial velocity profile in the daughter branch with the bifurcated angle of 30°. Velocity profile at a given section is skewed inward due to the centrifugal force in the curved flow resulting low velocity in the central region. Back flow is seen in the outer wall of the daughter branch where a recirculating zone is formed by the flow separation. Also, not shown in the figure, v-component of the velocity vector appears in the bifurcated region. The v-component does not appear in the main tube and far downstream of the branch. The complicated pressure variation in the bifurcated region is associated with the skewed velocity profile and separation bubble in the flow.

6.2 Effect of the power-law index of a non-Newtonian fluid

Effects of the power-law index n on the centerline velocity and pressure for the bifurcated angle of 30° are presented in Figs. 16 and 17, respectively. For the given value of n the changing shape of velocity profile along the axis is generally similar to that of Newtonian fluids. As the value of n decreases the centerline velocity also decreases, which implies that the velocity profile is becoming flatter in the central region for lower values of n. Steep decrease of velocity in the bifurcated

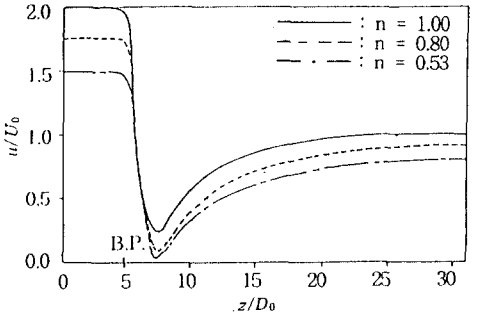

Fig. 16 Effect of the power-law index on the centerline velocity for the bifurcation angle of 30°

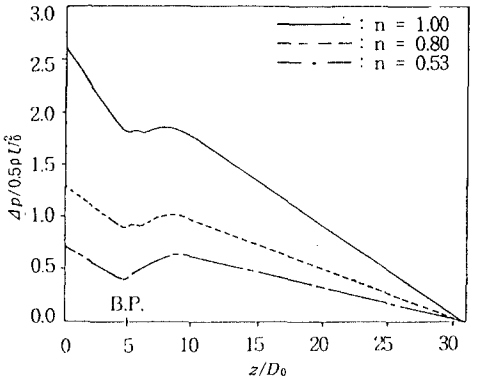

Fig. 17 Effect of the power-law index on the pressure variation for the bifurcation angle of 30°

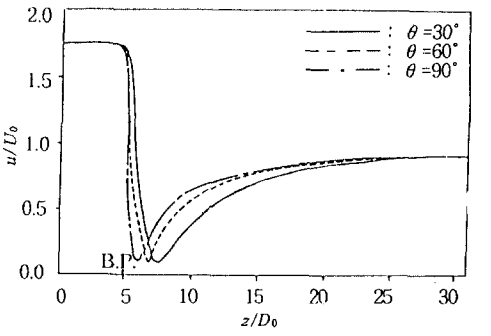

Fig. 18 Effect of the bifurcation angle on the centerline velocity for a non-Newtonian fluid of n =0.80

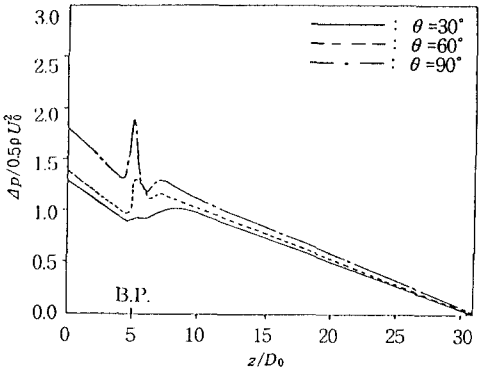

Fig. 19 Effect of the bifurcation angle on the pressure along the axis for a non-Newtonian fluid of n =0.80

region is more pronounced for the high value of n. Far downstream in the daughter branch, the velocity profile resumes its fully developed value just as in the main tube for the given value of n. Pressure variations in the upstream and downstream sides for the given value of n is just the same as the fully developed values. Dimensionless pressure drop for different index n is not identical either in the upstream or downstream side of the flow. The power-law index n of a non-Newtonian fluid plays a significant role on the pressure drop along the axis.

Effects of the bifurcated angle on the centerline velocity and pressure for the value of $n=0.80$ are shown in Figs. 18 and 19, respectively. Due to the nature of non-Newtonian fluids, the maximum velocity in the central region decreases when the value of n decreases. Effects of the bifurcation angle on the centerline velocity and pressure along the axis for the given n value is almost the same as those for a Newtonian fluid.

6.3 Effect of the diameter ratio

For Reynolds number of 400 and the bifurcation angle of 30°, effects of the diameter ratio on the centerline velocity and pressure variation of a Newtonian fluid are shown in Figs. 20 and 21, respectively. Diameter ratio is taken to be 1.0, 0.8, and 0.6 for comparative study. As the diameter ratio decreases the velocity in the branch increases and also, the pressure drop increases. For the diameter ratio of 0.6 the velocity in the daughter branch is larger than that of main tube due to restriction of the flow area. Abrupt change of velocity in the bifurcated region is seen in the

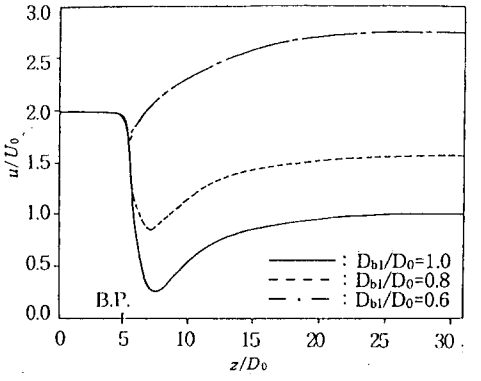

Fig. 20 Effect of the diameter ratio on the centerline velocity for a Newtonian fluid($\theta=30°$)

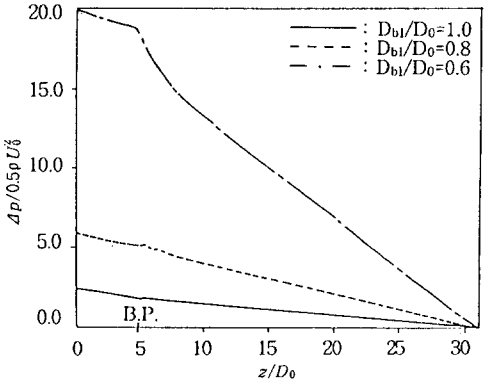

Fig. 21 Effect of the diameter ratio on the pressure along the axis for a Newtonian fluid($\theta=30°$)

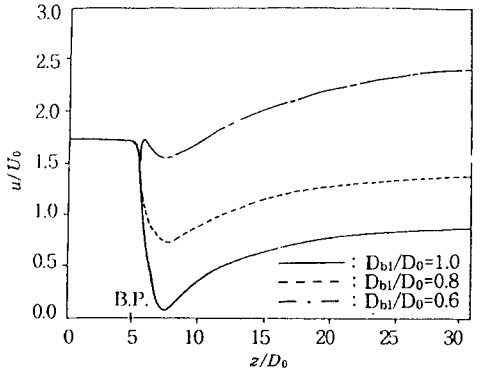

Fig. 22 Effect of the diameter ratio on the centerline velocity for a non-Newtonian fluid of n=0.80($\theta=30°$)

Fig. 20.

For Reynolds number of 400 and the bifurcation angle of 30°, effects of the diameter ratio on

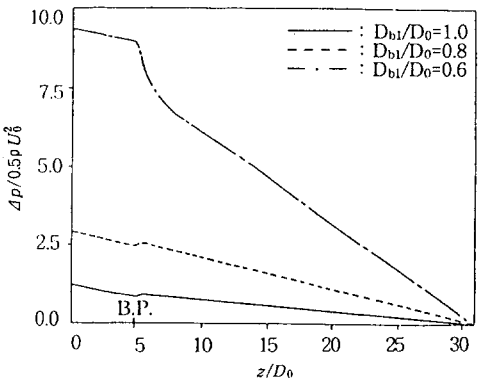

Fig. 23 Effect of the diameter ratio on the pressure along the axis for a non-Newtonian fluid of n=0.80($\theta=30°$)

the centerline velocity and pressure along the axis of a non-Newtonian fluid of $n=0.80$ are shown in Figs. 22 and 23, respectively. Effects of diameter ratio on the velocity and pressure are very much analogous to those on Newtonian fluids. Due to the difference of the apparent viscosity of non-Newtonian fluids the magnitude of the centerline velocity and the pressure drop are different depending upon the power-law index n.

7. Conclusions

① Among fluids studied, the rheological properties of aqueous Carbopol solution are similar to those of blood and the Carbolpol solution behaves quite similarly to the blood flow in the stenotic section.

② Blood and Carbopol solution show higher pressure drop along the axis and shorter reattachment length than those of water and sugar solution in the stenotic circular tube for the same Reynolds number.

③ Blood and Carbopol solution exhibit quite different pressure drop across the stenosis depending upon Reynolds numbers in the stenotic circular tube ; Pressure drop along the axis of blood is higher than that of Carbopol solution at $Re=50$, but the pressure drop of blood is lower than that of Carbopol solution at $Re=400$.

④ Centerline velocity variation of blood in the stenotic section with sudden contraction-sudden

expansion is larger than that in the stenotic section with gradual contraction-gradual expansion.

⑤ Both the dimensionless maximum velocity and the pressure loss decrease as the Reynolds number increases for blood flows in the stenotic section.

⑥ The centerline velocity for each bifurcation angle of 30°, 60° and 90° shows almost the same tendency for either Newtonian or non-Newtonian fluids. For the same bifurcation angle the pressure drop of a non-Newtonian fluid is smaller than that of a Newtonian fluid.

⑦ As the diameter ratio decreases, the centerline velocity in the daughter branch increases. The diameter effect on the centerline velocity and on the pressure loss of a power-law fluid along the axis is similiar to that of a Newtonian fluid.

Acknowledgment

Authors would like to express their appreciation to the Advanced Fluids Engineering Research Center, supported by the Korea Science and Engineering Foundation, for financial assistance.

References

Banerjee, R. K., 1992, A Study of Pulsatile Flows with Non-Newtonian Viscosity of Blood in Large Arteries, Ph. D. Thesis, Drexel University.

Chang, N. I., Suh, S. H. and Yoo, S. S., 1993, "Flow Analysis of Non-Newtonian Fluid in the Periodic Stenosed Tubes," *Proc. Fall meeting, KSME*, Vol. II, pp. 146～149.

Cho, Y. I., Back, L. H. and Crawford, D. W., 1985, "Experimental Investigation of Branch Flow Ratio, Angle, and Reynolds Number Effects on the Pressure and Flow Fields in Arterial Branch Models," *ASME J. Biomech. Engrg.*, 107, pp. 257～267.

Cho, Y. I. and Kensey, K. R. 1991, "Effects of Non-Newtonian Viscosity of Blood on Flows in a Diseased Arterial Vessel," : Part 1, Steady Flows, Biorheology, Vol. 28, pp. 241～262.

Choi, H. G. and Yoo, J. Y., 1992, "Finite Element Analysis of Two-Dimensional 90° Bifurcation Flow," *The 5th Asian Congress of Fluid Mechanics*, Taejon, Korea, pp. 1124～1127.

Khodadadi, J. M., Nguyen, T. M. and Vlachos, N. S., 1986, "Laminar Forced Convective Heat Transfer in a Two-Dimensional 90° Bifurcation," *Numerical Heat Transfer*, Vol. 9, pp. 677～695.

Lee. J. W. and Goo, J. H., 1993, "Inertial Deposition of Inhaled Particles in a Doubly-bifurcated Channel of the Human Respiratory Tract," *AFERC Report*, AFR-92-DO4, pp. 137～188.

Liepsch, D., Moravec, S., Rastagi, A. K. and Vlachos, N. S., 1982, "Measurement and Calculations of Laminar Flow in a Ninety Degree Bifurcation," *J. Biomech.*, Vol. 15, No. 7, pp. 473～485.

Milnor, W. R., 1989, *Hemodynamics*, 2nd Ed., Williams & Wilkins, London, pp. 51～57.

Morales, J. C. and Campo, A., 1993, "Analysis of Mixed Convection of a Non-Newtonian Fluid in a Cavity with a Uniformly Moving Wall," *The 6th Int. Symp. on Transport Phenomena in Thermal Engineering*, Seoul, Korea, Vol. II, pp. 39～42.

Nichols, W. W. and O'Rourke, M. F., 1990, *McDonalds' Blood Flow in Arteries*, 3rd Ed., Lea & Febiger, Philadelphia, pp. 12～53.

Pak, B., Cho, Y. I. and Choi, S. U. S., 1990, "Separation and Reattachment of Non-Newtonian Fluid Flows in a Sudden Expansion Pipe," *J. of Non-Newtonian Fluid Mech.*, Vol. 37, pp. 175～199.

Park, S. S. and Lee, H. S., 1992, "Pressure Drop for a Modified Power law Fluid Flow within Annular Ducts," *Proc., Spring meeting, KSME*, pp. 28～33.

Roh, H. W., Suh, S. H. and Yoo, S. S., 1993, "Flow Characteristics of Modified Power law Non-Newtonian Fluid in the Bifurcated Tubes," *Proc. Fall Meeting, KSME*, Vol. II, pp. 142～145.

Suh, S. H. and Yoo, S. S., 1993, "Flow Analysis of Power-law Non-Newtonian Fluid in the Stenosed Tube," *Proc., Summer Meeting, SAREK*, pp. 49～54.

Yoo, S, S., 1993, "Physical Properties and Heat Transfer in Tube Flows of Non-Newtonian

Fluids," *The 6th Int. Symp. on Tansport Phenomena in Thermal Engineering*, Seoul, Korea, Vol. II, pp. 61~70.

Yung, C. N., De Witt, K. J. and Keith, T. G. Jr., 1990, "Three Dimensional Steady Flow Through a Bifurcation," *ASME J. Biomech. Eng.*, Vol. 11, No. 2, pp. 189~197.